

## TERNARY SOLID-LIQUID EQUILIBRIA FOR CRYSTALLIZATION OF PHARMACEUTICAL COMPONENTS

M. H. Hamed<sup>1</sup>, L. Pison<sup>2</sup> and J-P. E. Grolier<sup>2\*</sup>

<sup>1</sup>Mechanical Engineering Department, K.N. Toosi University, Tehran, Iran

<sup>2</sup>Laboratory of Thermodynamics of Solutions and Polymers, Blaise Pascal University, Aubière, France

Isothermal titration calorimetry (ITC) has been used to develop a method to construct the solid-liquid equilibrium line in ternary systems containing the solute to precipitate and an aqueous mixed solvent. The method consists in measuring the heat of dissolution of a solid component (the solute) during successive additions of the liquid solvent. The cumulated heat, resulting from the successive heat peaks obtained for the different injections of known volumes of solvent, plotted vs. the ratio of the numbers of moles  $n_{\text{solvent}}/n_{\text{solute}}$  is represented by two nearly straight lines. The intersection of the two lines gives the solubility limit and the corresponding enthalpy of dissolution of the solute in the solvent.

Phase diagrams have been established at 303.15 K in binary mixed solvents ethanol-water over the whole concentration range for four components of pharmaceutical interest, namely: caffeine, nicotinamide, nicotinic acid and salicylic acid.

**Keywords:** caffeine, heat of dissolution, nicotinamide, nicotinic acid, salicylic acid, solid-liquid equilibrium, solubility, ternary systems, titration calorimetry

### Introduction

The present study takes place in the general approach regarding the design and the development of methods useful for the acquisition of thermodynamic data on phase equilibria in crystallization engineering. Crystallization is of particular interest since it constitutes the final step of purification of solids. Several methods have been designed in the past to obtain phase diagrams of a solid solute in a liquid medium acting as crystallization solvent; very often such methods were optical ones in which apparition (or disappearance), due to temperature or concentration changes, of a crystal was observed with the most appropriate optical device. Besides the advantage of observing the type of crystallinity, such methods are rather qualitative. More recently, precise quantitative techniques have been used to detect the solubility limit through the disappearance of the last crystal; in such dissolution techniques the solution concentration is observed continuously in following the change with temperature of a physical property of the solution like spectroscopic signal, density, vapour pressure, conductivity.

Calorimetric methods have been an invaluable tool for understanding many physical and chemical phenomena either in the early phases of process development, in biological applications, as well as for materials characterization. Like differential scanning

calorimetry (DSC), isothermal titration calorimetry (ITC) is very often used as analytical technique.

Titration calorimetry has been traditionally used for titration or acid-base reactions [1]. It is also currently used to study complex formation in pharmaceutical applications and binding effects in biophysical applications. Numerous examples of such investigations using ITC can be found in recent publications where different calorimeters have been used [2, 3]. In the last decade, the advent of several highly sensitive titration calorimeters has generated much interest in this technique [4–7]. However, titration calorimetry has been very rarely used to measure solubilization or dissolution of solid compounds; Smith *et al.* [8–10] have used ITC to establish solubility boundaries in complex systems like microemulsions. A rigorous control of temperature is essential in solubility phenomena then isothermal experimental techniques should be favoured. The construction of a phase diagram containing a solid solute and a liquid solvent is simply based on the determination of the solubility of the solid solute in the solvent. The solvent can be a pure liquid component or a liquid mixture for efficient solvent-antisolvent selective capability. The choice of selected solvents in crystallization processes rests on the knowledge of the solid phase contour of the product to precipitate in the presence of the solvent-antisolvent mixture. Since theoretical calculations are

\* Author for correspondence: J-Pierre.Grolier@univ-bpclermont.fr

not available so far to provide accurate prediction of the solubility limits of a solid component in binary mixtures, experimental determinations are necessary to establish solid-liquid phase equilibria in ternary systems. When the solute is an organic component the solvent is generally binary mixture water+a hydrophilic organic component. The thermodynamic study of the whole system is focused on the determination of the maximum of solubility of the solid solute, that is to say the solid-liquid line in the ternary system; this line which is the locus of the maximum solubility data points is readily obtained as of plot of those points. In this context, the solubility limit was determined by adding slowly (to remain at thermodynamic equilibrium) successive small increments of the binary solvent to a known (weighted) amount of the solid solute until the complete dissolution of the solid crystals. One of the important aspects of this work was the use of titration calorimetry to detect the dissolution of the solid in the binary solvent through the heat involved during each addition. Experimental setup and associated methodology have been previously used to establish ternary solid-liquid phase equilibria of vanillin, *o*-anisaldehyde and 1,3,5-trimethoxybenzene in water-alcohol binary mixtures [11]. For the present investigation phase diagrams have been established at 303.15 K over the whole concentration range for caffeine, nicotinamide, nicotinic acid and salicylic acid in water+ethanol binary mixtures.

## Experimental

### Chemicals

Caffeine (3,7-dihydro-1,3,7-trimethyl-1H-purine-2,6-dione) polymorphic form 1 monoclinic type (attested by DSC and XRD) with 98.5 mol% purity, nicotinamide (3-pyridine-carboxamide, or niacinamide) with 98 mol% purity, nicotinic acid (3-pyridinecarboxylic acid, or niacin, or vitamin B3) with 99.5 mol% and salicylic acid (2-hydroxybenzoic acid) with 99 mol% purity respectively were provided by (Fine Chemicals) Acros Organics France; ethyl alcohol absolute RE was provided by Carlo Erba France. All chemicals were used without further purification. Solutions were prepared by mass using freshly bidistilled water.

### Instrumentation

The titration calorimeter, Titrys model, commercialized by Setaram was used to perform the solubility measurements. The calorimeter is built according to the Calvet principle. The calorimetric block whose

temperature can be regulated to  $\pm 20$  mK houses two thermopiles in which are placed the measuring and reference cells respectively. The differential detection allows detecting heat effects with 0.1  $\mu$ W sensitivity. The instrument can be operated in the temperature range from 303.15 to 333.15 K. For this application the calorimeter (see a schematic view of the calorimeter in Fig. 1a) presents a double interesting feature: in each cell an active volume from 1 up to 12 cm<sup>3</sup> can be used and the content of each cell can be stirred by means of a small magnetic bar activated by a single small motor which ensures the same (adjustable) stirring speed in both cells. The calorimeter can be fed with an injection system Dual Syringe Pump Model 33 from Harvard, composed of two identical syringe pumps mounted on a dual carriage in such a way that identical volumes delivered by stainless capillaries can be injected simultaneously at exactly the same rate in both cells; during each injection the corresponding heat effect is recorded as shown in Fig. 1b. The injection system is entirely programmable and computer controlled. In order to ensure a better control of the volumes delivered by the pumps, the whole assembly, syringe pumps and their carriage/holder, were placed in a small air bath thermostated to  $\pm 50$  mK. Before injection in the calorimetric cells, liquids coming from the pumps are further thermostated as the feeding capillaries are coiled in two small thermostats placed inside the calorimetric block on top of each cell (see details in Fig. 2).

### Experimental procedures

An initial mass, 0.05–2.50 g depending on the type of solid, of finely hand-ground (in a mortar) crystallized powder is placed in the measuring cell. The two syringe pumps are filled with the same water-alcohol

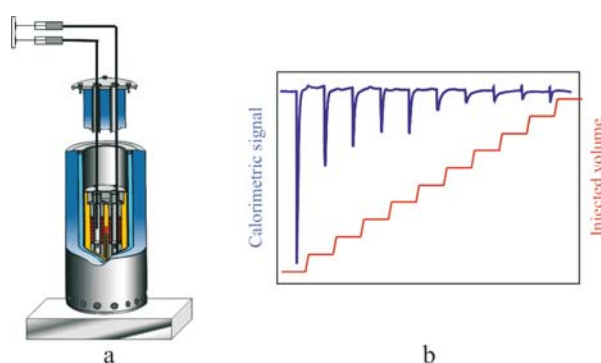


**Fig. 1** a – General view of the Titrys titration calorimeter, showing the differential mounting of the thermopiles housing the calorimetric cells, the thermostated head (in an upper position) and the injection dual syringe system; b – Calorimetric signal vs. injected volume of solvent, showing thermal traces of heat effects obtained upon successive additions during an isothermal run

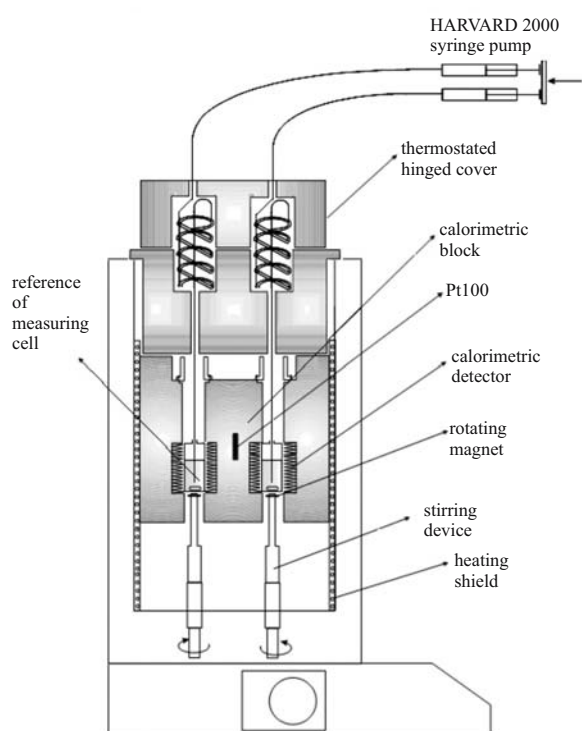


**Fig. 2** Schematic view of the calorimeter showing the main features of the instrument, namely: dual syringe pump injection system, stainless capillary tubings, coiled capillaries cylinders which are inserted in the thermostated head of the calorimeter, measuring and reference cells and their individual stirring devices

solution of known composition. A dissolution run consists in adding the same volume of the solution simultaneously in both cells. The heat repeatedly evolved during each addition is due to the heat of dissolution of part of the solid in the small amount of added solution; this is directly given by the differential heat flux recorded upon injection of the solution. Typically, each injection consists in adding  $0.20 \text{ cm}^3$  of solution at the rate of  $0.10 \text{ cm}^3 \text{ min}^{-1}$  and a complete run is achieved after an average of 10 successive additions. The volume for an injection may vary from  $0.04$  to  $2.00 \text{ cm}^3$  of solution at the rate between  $0.02$  and  $0.70 \text{ cm}^3 \text{ min}^{-1}$ . Each run yields a series of heat peaks vs. time (as shown in Fig. 1b). The cumulative sums  $\Delta H$  of heat effects (the actual total peak areas) divided by  $n_1$  ( $n_1 = n_{\text{solute}}$ , initial number of moles of solute) are plotted vs.  $\alpha = n_{\text{solvent}}/n_{\text{solute}}$  which represents the ratio of the number of moles of solvent to the number of moles of the solute. Each dissolution/dilution run yields the type of plot shown in Fig. 3. Typically each experiment is composed of two parts. First an increase of  $\Delta H$  represented by a linear function with  $\alpha: \Delta H/n_1 = A_1\alpha$ . Then, when the entire solid has been completely solubilized, the second part which is simply related to the heat of dilution of the medium, is

generally well represented by a polynomial of the form:

$$\Delta H n_1 = A'_0 + A'_1 \alpha + A'_2 \alpha^2 \quad (1)$$

The coefficients  $A_1, A'_0, A'_1, A'_2$  were determined by linear regression. The intersection of the two parts gives the enthalpy of dissolution for a given ratio  $\alpha_S$  at saturation, Eq. (2):

$$A_1 \alpha_S = A'_0 + A'_1 \alpha_S + A'_2 \alpha_S^2 \quad (2)$$

From  $\alpha_S$  at saturation, the composition of the ternary system at saturation can be determined as follows:

$$\alpha_S = n_{\text{solvent}}/n_1 = (n_2 + n_3)/n_1 = (x_2 + x_3)/x_1 \quad (3)$$

where  $n_i$  is the number of moles of each component.

Since  $x_1 + x_2 + x_3 = 1$  one can finally write:  $\alpha_S = (1 - x_1)/x_1$  and  $x_1 = 1/(\alpha_S + 1)$ ,  $x_2 = x_{2,S}(1 - x_1)$ , and  $x_3 = x_{3,S}(1 - x_1)$ , respectively, where  $x_{2,S}$  and  $x_{3,S}$  are respectively the mole fractions of components 2 and 3 in the binary mixture water+alcohol. Remarkably, when  $\alpha = \alpha_S$  the heat of dissolution in the mixed binary solvent, that is the enthalpy of solution at saturation, is obtained from in Eq. (1).

The dissolution runs are made in such a way as to cover the whole concentration of the binary aqueous mixture. The original raw data are respectively the amount (in weight  $w_1$ ) of solute 1, the injected volumes of the aqueous mixed solvent (water+alcohol) in which the amount  $w_2$  of water is known as well as the amount  $w_3$  of alcohol. Densities of water-alcohol mixtures were taken from literature [12] to evaluate

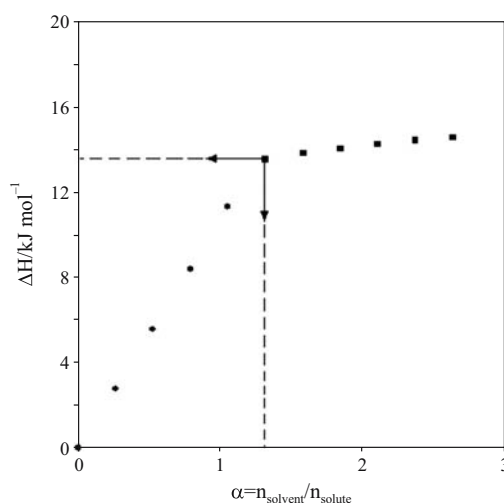


**Fig. 3** Plot of cumulated thermal effects,  $\Delta H/n_1$  (in  $\text{J mol}^{-1}$ ), vs.  $\alpha = n_{\text{solvent}}/n_1$ , obtained during a run, showing the initial dissolution  $\bullet$  – of the solid solute followed by the dilution  $\blacksquare$  – of the solution. The intersection gives the enthalpy of dissolution and the ratio  $\alpha_S$  at saturation;  $n_1$  is the initial number of moles of solute  $n_{\text{solute}}$  placed in the measuring cell

the respective quantities of water and alcohol in the injected volumes of solvent. From the different weights  $w_i$  the corresponding mole fractions ( $x_1$ ,  $x_2$ ,  $x_3$ ) were calculated; they constitute the experimental data to be treated in order to get the fitting equations to represent the solid-liquid equilibrium lines for the different systems. The ternary plots ( $x_1$ ,  $x_2$ ,  $x_3$ ) on Figs 4 to 7 are then constructed from the actual experimental mole fractions which correspond to the individual coordinates of the different intersections (Fig. 3).

## Results and discussion

For the different investigated systems the experimental mole fractions  $x_1$ ,  $x_2$  and  $x_3$ , representing component 1, the solid solute, component 2, water (H<sub>2</sub>O), and component 3, ethanol (EtOH), respectively are listed in Table 1. Graphical representation of the measured data are shown in Figs 4–7. In these Figures the

smoothed curves have been obtained through the procedure described in what follows. The original raw data are respectively the amount (in weight  $w_1$ ) of solute 1, the volume of the aqueous mixed solvent (water+alcohol) in which the amount  $w_2$  of water is known as well as the amount quantities of water and alcohol in the injected volumes of solvent. From the different weights  $w_i$  the corresponding mole fractions were calculated; they constitute the experimental data to be treated in order to get the fitting equations to represent the solid-liquid equilibrium lines for the different systems. Firstly, a plot of  $x_1$  vs.  $x_2$  was fitted with the following polynomial  $y$ :

$$y=x_1=f(x_2)=\sum_{i=0}^n a_i (1-x_2)^i \quad (4)$$

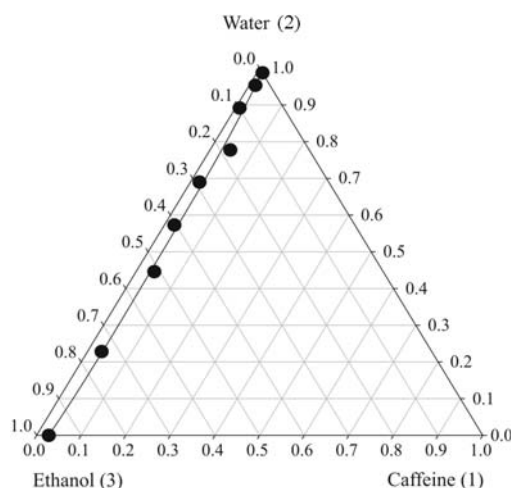
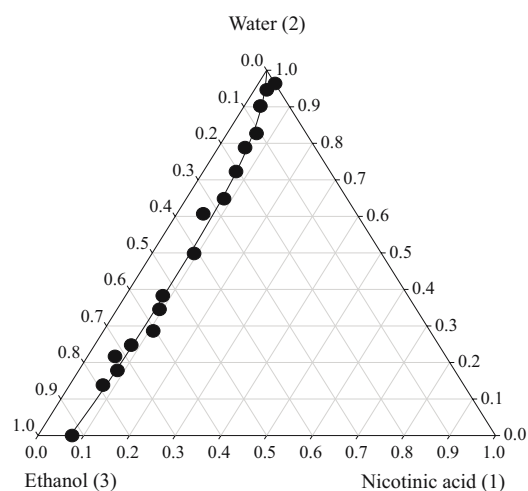
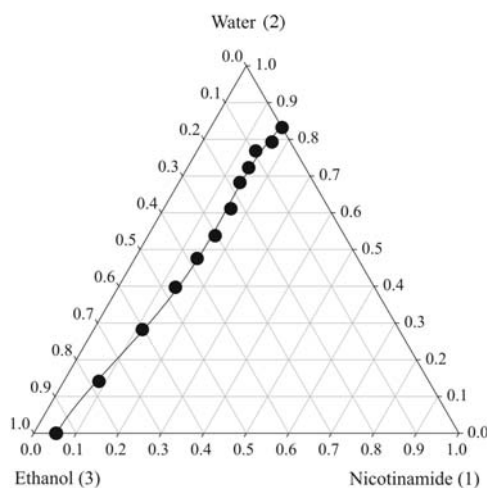
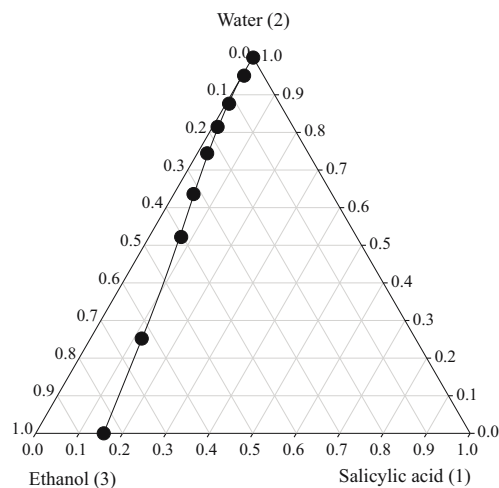
Coefficients  $a_i$  were adjusted to give the best fit. Secondly, using polynomial  $y$  a table of numerical values  $X_3$  is generated as a function of  $X_2$ ,  $X_3=f(X_2)$ , at rounded values of  $X_2$  (e.g.  $0 \leq X_2 \leq 1$  at 0.05 increments)

**Table 1** Experimental mole fractions at 303.15 K of the different components in the ternary systems corresponding to the data points in Figs 4 to 7

Caffeine (1)+H <sub>2</sub> O (2)+EtOH (3)			Nicotinamide (1)+H <sub>2</sub> O (2)+EtOH (3)		
$x_1$	$x_2$	$x_3$	$x_1$	$x_2$	$x_3$
0.0124	0.9876	0.0000	0.1680	0.8320	0.0000
0.0136	0.9536	0.0329	0.1639	0.7926	0.0435
0.0089 <sub>7</sub>	0.8918	0.0993	0.1378	0.7681	0.0941
0.0453	0.7775	0.1773	0.1441	0.7226	0.1333
0.0201	0.6899	0.2900	0.1435	0.6823	0.1742
0.0221	0.5731	0.4048	0.1580	0.6110	0.2310
0.0409	0.4458	0.5153	0.1577	0.5376	0.3047
0.0315	0.2283	0.7402	0.1462	0.4757	0.3781
0.0274	0.0000	0.9726	0.1346	0.3972	0.4683
			0.1144	0.2820	0.6036
			0.0828	0.1411	0.7760
			0.0534	0.0000	0.9466
			0.0520	0.0000	0.9480
Nicotinic acid (1)+H <sub>2</sub> O (2)+EtOH (3)			Salicylic acid (1)+H <sub>2</sub> O (2)+EtOH (3)		
$x_1$	$x_2$	$x_3$	$x_1$	$x_2$	$x_3$
0.0364	0.9636	0.0000	0.0012 <sub>1</sub>	0.9988	0.0000
0.0267	0.9464	0.0269	0.0042 <sub>7</sub>	0.9506	0.0451
0.0350	0.9020	0.0630	0.0069 <sub>2</sub>	0.8762	0.1169
0.0641	0.8270	0.1089	0.0112	0.8145	0.1742
0.0585	0.7882	0.1533	0.0224	0.7442	0.2334
0.0714	0.7225	0.2061	0.0452	0.6360	0.3188
0.0825	0.6481	0.2694	0.0738	0.5217	0.4044
0.0577	0.6068	0.3356	0.1181	0.2518	0.6301
0.0919	0.4982	0.4099	0.1566	0.0000	0.8434
0.0815	0.3825	0.5360			
0.0927	0.3454	0.5618			
0.1082	0.2855	0.6036			
0.0800	0.2474	0.6726			
0.0601	0.2165	0.7234			
0.0843	0.1783	0.7374			
0.0730	0.1379	0.7891			
0.0745	0.0000	0.9255			

**Table 2** Coefficients of the fitting Eq. (8) and corresponding standard deviations  $\sigma$  used to represent the smoothed curves in Figs 4 to 7

Systems	$a_0$	$a_1$	$a_2$	$a_3$	$a_4$	$\sigma$
Caffeine+H <sub>2</sub> O+EtOH	0.0080	0.1405	-0.3478	0.4205	-0.1942	0.0143
Nicotinamide+H <sub>2</sub> O+EtOH	0.2896	-1.2912	4.0978	-5.2591	2.2164	0.0081
Nicotinic acid+H <sub>2</sub> O+EtOH	0.0253	0.1488	1.1467	-0.5485	0.3001	0.0128
Salicylic acid+H <sub>2</sub> O+EtOH	–	-0.0370	0.7286	-0.8850	0.3498	0.0031

**Fig. 4** Ternary plot for the system caffeine (1)+water (2)+ethanol (3) at 303.15 K, ●, this work; the fitting curve represents Eq. (4), with coefficients of Table 2**Fig. 6** Ternary plot for the system nicotinic acid (1)+water (2)+ethanol (3) at 303.15 K, ●, this work; the fitting curve represents Eq. (4), with coefficients of Table 2**Fig. 5** Ternary plot for the system nicotinamide(1)+water (2)+ethanol (3) at 303.15 K, ●, this work; the fitting curve represents Eq. (4), with coefficients of Table 2**Fig. 7** Ternary plot for the system salicylic acid (1)+water (2)+ethanol (3) at 303.15 K, ●, this work; the fitting curve represents Eq. (4), with coefficients of Table 2

using the relation:  $X_3=1-x_1-X_2$ , where  $x_1=y=f(X_2)$  as given by Eq. (5) and  $x_1+X_2+X_3=1$ .

This 'normalization' step allows then to draw the smoothed curves in Figs 4–7. Equation (4) is the actual fitting equation of the experimental data points. The best fit has been obtained using a SigmaPlot software which gives the solubility maximum of the solid in the optimal composition of the aqueous mix-

ture (Table 3). The coefficients  $a_i$  and corresponding standard deviations  $\sigma$  are listed in Table 2.

## Conclusions

The four components investigated are generally slightly soluble in the two liquids, water and ethanol.

**Table 3** Mole fractions of the 3 components in each ternary system corresponding to the maximum of solubility at 303.15 K of the solid solute in the optimal composition of the binary aqueous mixture

Systems	$x_1$ (max)	$X_2$ (H <sub>2</sub> O)	$X_3$ (ROH)
Caffeine+H <sub>2</sub> O+EtOH	0.0337	0.2400	0.7263
Nicotinamide+H <sub>2</sub> O+EtOH	0.1645	0.8301	0.00046
Nicotinic acid+H <sub>2</sub> O+EtOH	0.0840	0.3800	0.5360
Salicylic acid+H <sub>2</sub> O+EtOH	0.1564	0.0000	0.8436

Remarkably, nicotinamide is more soluble than nicotinic acid and therefore more alcohol is necessary to solubilize (then for recrystallizing) nicotinic acid. The different shapes of the solid-liquid equilibrium lines result from the differences in chemical structures of the solutes.

In conclusion, isothermal titration calorimetry can be recommended as a convenient technique to obtain not only a qualitative description of solid-liquid phase diagrams in ternary systems, but also precise concentrations of the components along the solid-liquid line. The fitting equations developed to represent this line can be used for engineering calculations.

### Acknowledgements

The authors express their appreciation to Prof. B. Legendre (Faculté de Pharmacie, Châtenay Malabry, France) for making the DSC and XR diffraction measurements to establish the caffeine crystallographic form.

### References

- 1 S. L. Randzio, *Chem. Soc. Rev. Annu. Rep. Prog. Chem. C.*, 27 (1998) 433.
- 2 N. Markova and D. Hallen, *Anal. Biochem.*, 331 (2004) 77.
- 3 I. Wadsö, *Chem. Soc. Rev.*, 26 (1997) 383.
- 4 M. M. Pierce, C. S. Raman and B. T. Nall, *Methods*, 19 (1999) 213.
- 5 T. Wiseman, S. Williston, J. F. Brandts and L. N. Lin, *Anal. Biochem.*, 179 (1989) 131.
- 6 E. Freire, O. L. Mayorga and M. Straume, *Anal. Chem.*, 62 (1990) 950.
- 7 D. S. Gill, D. J. Roush, K. A. Shick and R. C. Willson, *J. Chromatogr. A.*, 715 (1995) 81.
- 8 D. H. Smith and G. C. Allred, *J. Colloid Interface Sci.*, 124 (1988) 1999.
- 9 D. H. Smith and G. L. Covatch, *J. Colloid Interface Sci.*, 162 (1994) 372.
- 10 D. H. Smith and G. L. Covatch, *J. Colloid Interface Sci.*, 171 (1995) 112.
- 11 M. H. Hamed, B. Laurent and J-P. E. Grolier, *Thermochim. Acta*, 445 (2006) 70.
- 12 G. C. Benson and O. Kiyohara, *J. Sol. Chem.*, 9 (1980) 791.

DOI: 10.1007/s10973-006-7951-1